Nucleation, growth and structural development of mylonitic shear zones in granitic rock

PETER P. CHRISTIANSEN* and DAVID D. POLLARD

Department of Geological and Environmental Sciences, Stanford University, Stanford, CA 94305, U.S.A.

Abstract—Well-exposed shear zones in granitic rock of the Sierra Nevada are preserved in various degrees of development, facilitating interpretation of the mechanisms of shear-zone nucleation and growth. Field relations suggest that these shear zones formed by shear localization within pre-existing aplite dikes that served as tabular zones of inherent weakness. Crossing dikes provide a measure of the offset at several points along the shear zones. Apparently, the shear zones grew in width as they accumulated offset, and propagated longitudinally by end-to-end linkage of approximately coplanar aplite dike segments. Propagation caused discontinuous dikes or dike segments to be joined, giving the shear zones a forked, or eye-shaped, trace pattern. Some shear zones have developed opening fractures at their tips, analogous to the splay fractures that form near the tips of small faults. These shear zones provide an excellent opportunity to study the processes involved in natural shear-zone formation in granitic rocks where shear is localized along pre-existing zones of inherent weakness. They may serve as useful analogs for the growth and development of larger-scale faults that involve ductile shearing. © 1997 Elsevier Science Ltd.

INTRODUCTION

Conceptual models of fault zones that transect significant portions of the crust commonly include zones of distributed shear deformation in the lower–middle crust (Lachenbruch and Sass, 1973; Thatcher, 1975a,b; Sibson, 1977; Prescott and Nur, 1981; Passchier, 1982; Bonafede, 1990). Faulting in these models is accommodated in the upper crust (the seismogenic zone) by slip along relatively discrete surfaces or zones of discrete faults, whereas in the middle and lower crust shear deformation is distributed over more diffuse zones and may involve plastic deformation. In the transition between the two regimes, deformation along discrete surfaces and over distributed zones may be overprinted (Sibson, 1980; Passchier, 1982; Hobbs *et al.*, 1986). That major upper-crustal faults are continuous with shear zones in the middle and lower crust is consistent with the observed uniformity of the long-term displacement rates seen across major plate boundaries (Savage and Burford, 1973). This may also be true in some intraplate settings (Zoback *et al.*, 1985).

An inferred change in deformation mechanisms with depth may explain the lack of earthquakes beneath seismically active fault systems. This transition is almost certainly influenced by temperature (Byerlee, 1968; Brace and Byerlee, 1970), although other factors are thought to contribute. Using a lithospheric rheology, derived from laboratory deformation studies, the transition has been related to the change from pressure-sensitive frictional sliding to temperature-dependent plasticity (Sibson, 1982; Kirby, 1985; Dragoni *et al.*, 1986; Dragoni and Pondrelli, 1991). In addition to this change, the depth distribution of earthquakes may be influenced by a change from velocity-strengthening to velocity-weaken-

ing behavior (Tse and Rice, 1986; Scholz, 1988). Shear zones underlying seismogenic fault zones may play a role in the long-term cycle of strain accumulation and release (Thatcher, 1975b; Prescott *et al.*, 1979), and thus be a factor in nucleating earthquakes (Sibson, 1982; Ohnaka, 1992). Stress transfer between the seismogenic layer and shear zones in the middle and lower crust has also been invoked to explain phenomena such as post-seismic creep (Cohen, 1981; Bonafede, 1990).

Because of their potential importance for fault-zone tectonics, for the loading of the seismogenic layer and for the overall understanding of faulting phenomena in general, shear zones have been a prominent subject in the structural geology literature for decades. Despite this, several questions remain about the formation and evolution of shear zones that cannot be addressed solely by laboratory studies, as these are limited to small samples. For example, how do shear zones initiate and how do they propagate? For this reason, the field study of exhumed shear zones remains critical.

Several workers have interpreted shear-zone fabrics in terms of the change in physical conditions across the ductile–brittle transition. As polycrystalline rocks, such as granite, are sheared in a fault zone, deformation textures progress from protomylonite to ultramylonite (Sibson, 1977; White *et al.*, 1980; Simpson, 1985). Early in this development, rock strength is determined by the proportions of various minerals such as quartz and feldspar (Jordan, 1988). Once deformation has progressed to the point that a penetrative mylonitic foliation develops, the bulk strength of the rock will decrease and may approach the strength of the weakest component (Tullis, 1990). The corresponding textural transition is related to the transition from the pressure-sensitive regime dominated by cataclasis and frictional sliding to the temperature-sensitive regime dominated by intra-

*Present address: Mineral Resources Development Inc., 1710 S Amphlett Blvd #302, San Mateo, CA 94402, U.S.A.

crystalline plasticity and mylonitization (Sibson, 1977, 1982).

In addition to physical conditions, shear-zone structures and fabrics are essential for interpreting the mechanisms by which shear zones nucleate and propagate. The nucleation of shear zones requires that shear strain be localized. This can result from a plastic instability (Poirier, 1980) or from material heterogeneities such as pre-existing fractures (Segall and Simpson, 1986; Tullis et al., 1990). In the later case, shear localization is attributed to various strain-softening mechanisms including recrystallization (Schmid, 1975; Tullis et al., 1990), chemical weakening caused by the introduction of fluids (Mitra, 1978; Beach, 1980; Kronenberg et al., 1990) or other mechanical means (Wojtal and Mitra, 1986). One of the principal softening mechanisms is thought to be a reduction in grain size due to either cataclasis or to various types of syn-kinematic recrystallization (Nicolas and Poirier, 1976; White et al., 1980).

A detailed understanding of shear-zone nucleation and propagation remains elusive because: (1) crustal rocks respond to deformation in a complex way under varying conditions of pressure, temperature and strain rate, producing a wide variety of shear-zone types each with a unique geological history; (2) exposure of natural shear zones is often incomplete, commonly being restricted to two-dimensional planes; and (3) evidence for the early history of nucleation and propagation is commonly destroyed by later deformation. As a result, many previous studies of shear zones have been restricted to investigating the distribution of strain or displacement in profiles across various classes of shear zones (e.g. Coward, 1976; Ramsay, 1980; Simpson, 1983a; Passchier, 1986), and only occasionally has the deformation near shear-zone terminations been studied (Coward and Potts, 1983; Simpson, 1983b).

The purpose of the present paper is to document the structural characteristics of a set of natural mylonitic shear zones which may serve as useful analogs to active faults at mid-crustal depths. Exposure of the shear zones is very good, allowing direct observation, measurement and sampling of the structures over much of their length, including shear-zone terminations at both high and low angles to the relative-offset vector. In addition, because several stages in the development of these shear zones are preserved, we can interpret the processes involved in their nucleation and subsequent propagation. A mechanical analysis of these processes is discussed by Christiansen (1995).

GEOLOGICAL SETTING

We have mapped and sampled shear zones of various sizes and in various degrees of development throughout an area of approximately 1 km^2 straddling the contact between the Lake Edison and Mono Creek plutons,

central Sierra Nevada (Fig. 1). The shear zones are mostly restricted to this area, although we have found scattered examples within the interior of the Mono Creek pluton. Because the geological history of this area is described elsewhere (Lockwood, 1975; Lockwood and Lydon, 1975; Bateman, 1992; Christiansen, 1995) only a brief outline is given here.

The Lake Edison pluton is a fine- to medium-grained hornblende–biotite granodiorite that is intruded by the younger Mono Creek Granite. The typical Mono Creek lithology is a coarsely porphyritic granite with 1–2.5 cm alkali-feldspar megacrysts in a matrix containing biotite with minor hornblende and sphene (Lockwood and Lydon, 1975; Bateman, 1992).

Uranium–lead zircon dates of ~90 Ma on the Lake Edison and Mono Creek plutons (Stern et al., 1981) provide a maximum age constraint for the shear zones (Fig. 1). The shear zones are cross-cut and offset by mineralized faults and fault zones that contain rare hydrothermal muscovite. This muscovite yields $^{40}Ar/^{39}Ar$ dates as young as 79.2 ± 0.8 Ma (Segall et al., 1990), providing a minimum age constraint for the shear zones: the shear zones formed at most 11 Ma after crystallization of the host plutons. Because it is unlikely that the shear zones formed at a depth greater than the crystallization depth of the host granitoid, and because there is no evidence for significant regional exhumation of the batholith within this time interval (Bateman et al., 1963; Huber, 1981), the shear zones probably formed at a depth close to the crystallization depth. Depth of emplacement of the plutons is estimated to be ~4–15 km, based on pressure estimates of 100–400 MPa determined by amphibole geobarometry (Ague and Brimhall, 1988).

By analogy with laboratory deformation of quartzo-feldspathic rocks (Tullis, 1990), formation of the shear zones at temperatures of 300–450°C is consistent with the observed crystal–plastic behavior of quartz, and the brittle to perhaps modestly crystal–plastic behavior of feldspar (see below). As deformation at this temperature is below the argon closure temperature in hornblende (~500°C), deformation probably took place after ~85 Ma. This is based on 85 Ma K–Ar hornblende dates reported by Everden and Kistler (1970), adjusted to the decay constants recommended by Steiger and Jäger (1977).

DESCRIPTION OF THE SHEAR ZONES

Aplite and pegmatite dikes lie in a variety of orientations throughout the study area. Individual dikes vary in width from <5 to ~200 cm, averaging 8 cm. Cross-cutting relations reveal at least two distinct generations of dikes: an older set of mixed aplite and pegmatite dikes that strikes 140°–180°, essentially parallel to the contact between the Lake Edison and Mono Creek plutons, and a younger set with some pegmatite, but predominantly aplite, that strikes 0°–130°. Where dikes of the younger
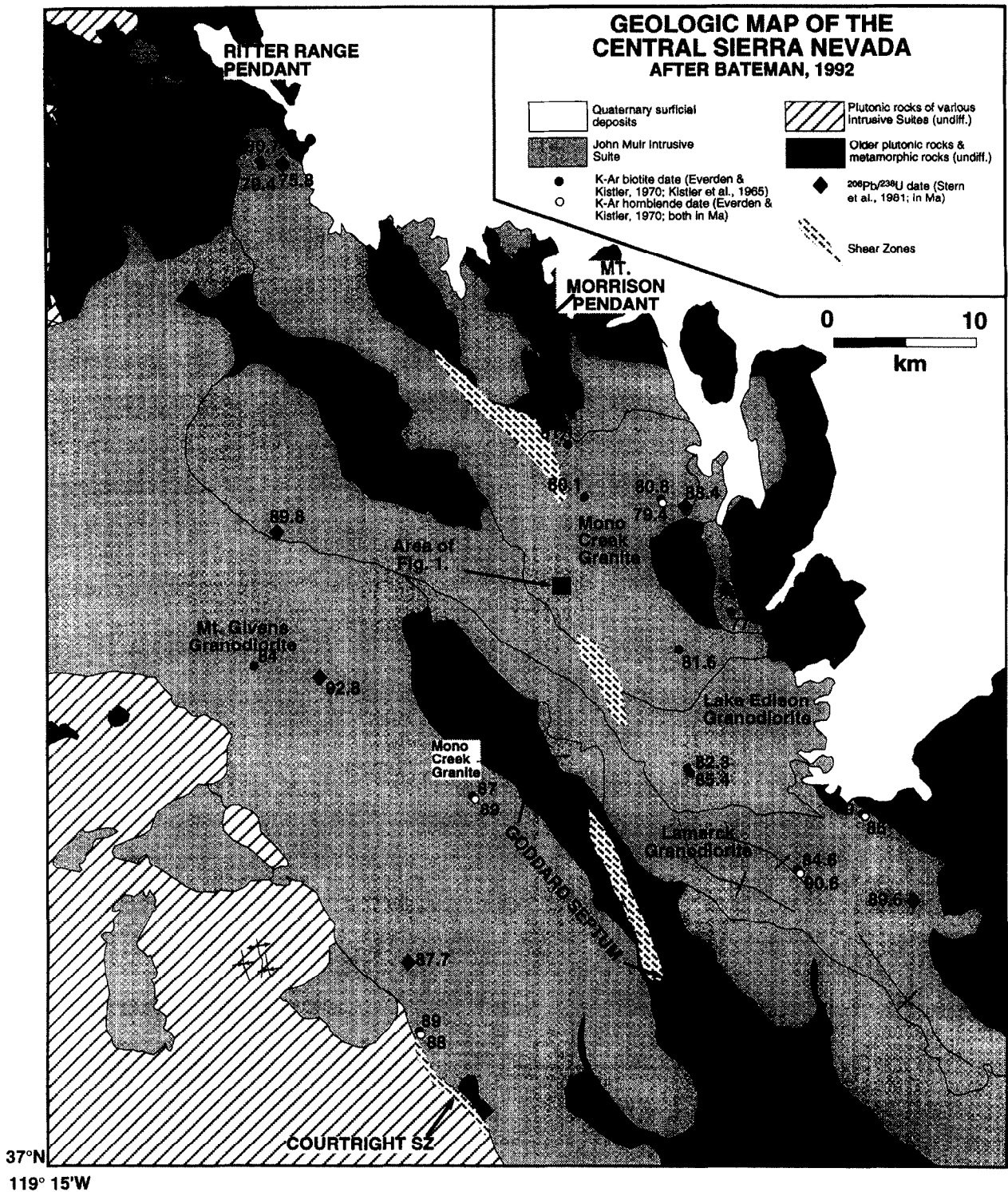
Fig. 1. Geological map of the central Sierra Nevada, simplified from Bateman (1992). Regional shear zones are shown in a hachured pattern. Line segments show the trace of foliation. Other structural symbols include normal faults (balls on the down-thrown side) and fold axes. Box in the center shows the approximate location of the 'White Bark' outcrop (Fig. 2).

set strike 090° ± 20° they are sheared, showing the development of mylonitic textures and left-lateral offset of cross-cutting markers. These dikes have localized shear strain and thus have served as the nucleation sites for mylonitic shear zones.

In order to describe the shear zones in more detail, we focus on an area we call the White Bark outcrop (Fig. 2). Shear zones here range in width from 3 to 10 cm, averaging 4.5 cm, and range in length from 2 to > 200 m. The largest shear zone in the area (the 'South
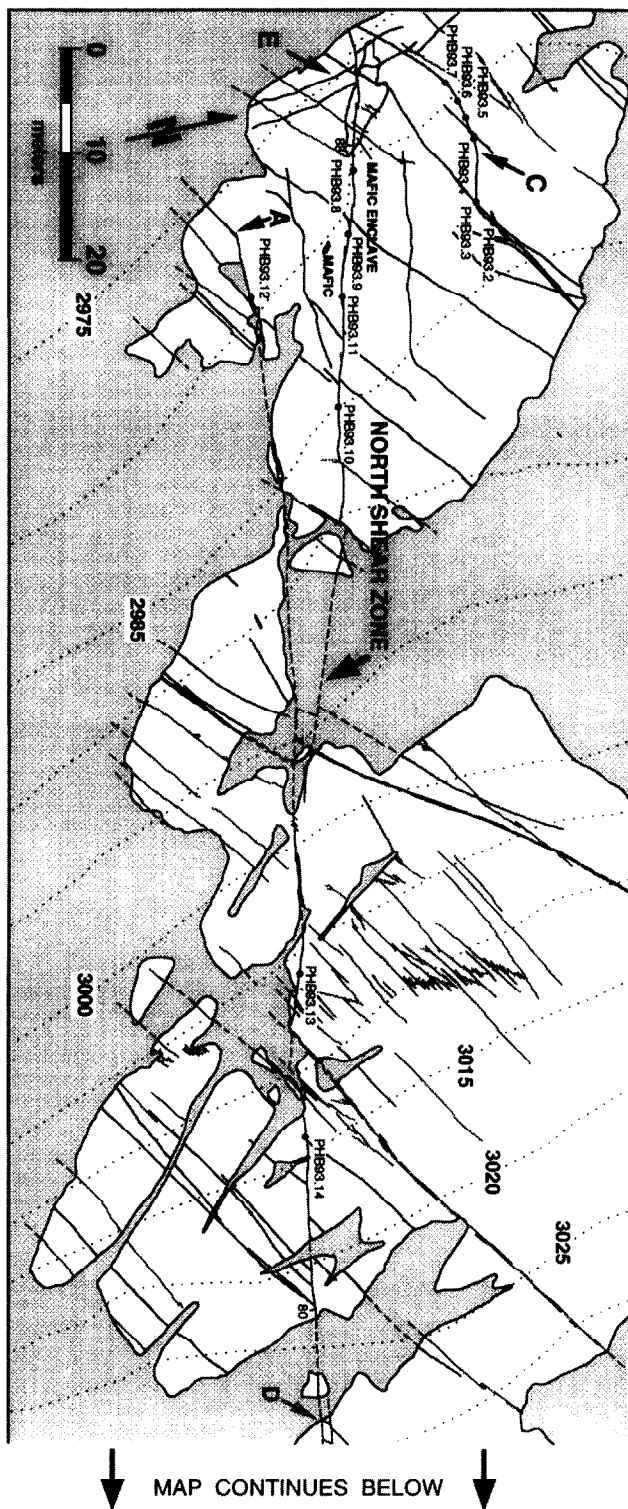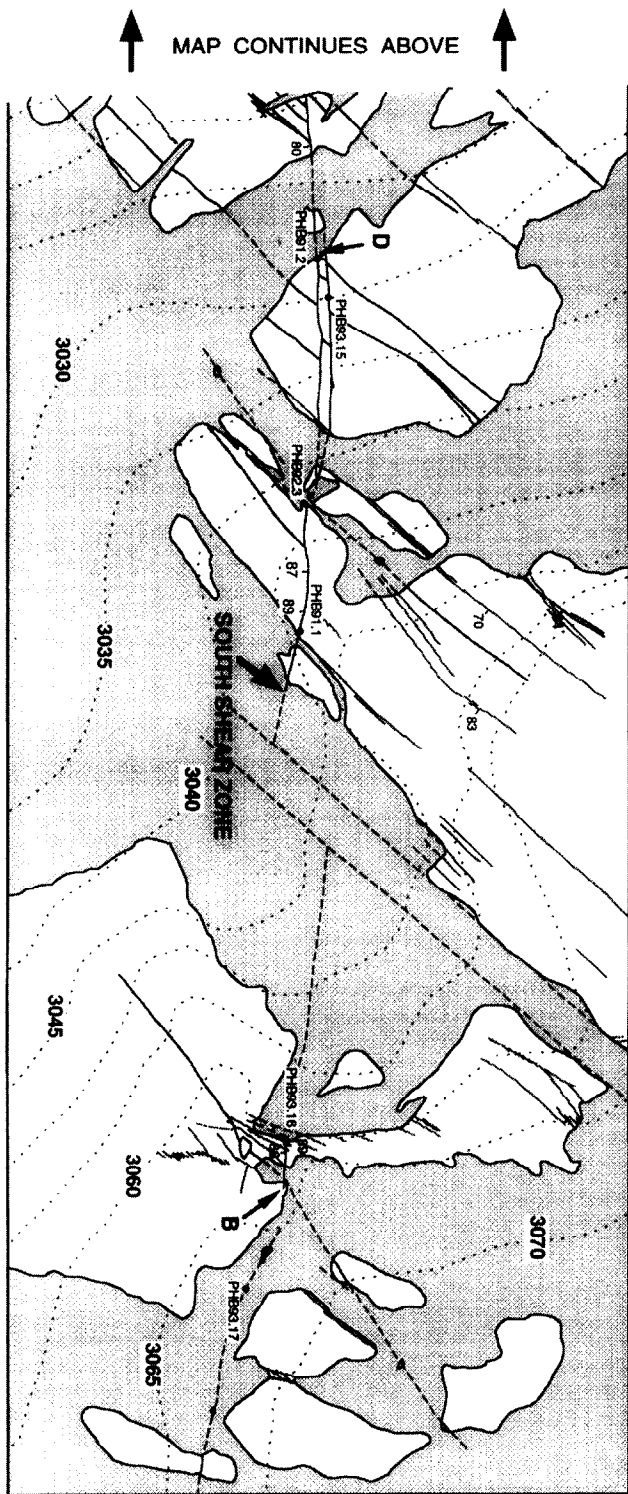
shear zone', SSZ, Fig. 2) is at least 235 m in outcrop length and is exposed at the surface over ~90 m of vertical relief. Relative offset across the zone is predominantly left-lateral strike-slip. The termination of the zone at point A is a lateral tip-line, while up-slope to the east a second termination at point B is near the upper tip-line of the shear zone. The eastern lateral tip-line of the zone is not exposed. A second large zone (the 'North shear zone', NSZ, Fig. 2) is at least 60 m long and is exposed over ~25 m of vertical relief. The western lateral tip-line is not exposed, so its extent is unknown.

Rock inside all but the lowest-strain shear zones is fine-grained (1–250 μm) mylonite that occasionally encloses 1–2 mm feldspar porphyroclasts. Less well-developed shear zones show a streaky black foliation parallel with the dike margins. Where the grain size is larger, especially near the shear-zone margins, quartz shows undulose extinction, subgrains and a lattice-preferred orientation suggestive of polygonization and dynamic recrystallization. Feldspar grains are deformed primarily by brittle fracture, but occasionally they show bent cleavage and undulose extinction. Further investigation is needed to determine the detailed nature of deformation in feldspar grains.

Along most of their length the boundaries of the shear zones are quite sharp, so that essentially undeformed rock with a shear strain ≪ 1 lies within a few millimeters of highly deformed rock with a shear strain up to ~100 (Fig. 3a). This is in distinct contrast to some descriptions of shear zones wherein strain increases gradually from the wallrock into the center of the zone (Ramsay and Graham, 1970; Ramsay, 1980; Coward and Potts, 1983; Simpson, 1983b; Segall and Simpson, 1986). Occasionally, undeformed host-rock grades continuously into S–C-type mylonite, then into the fine-grained mylonite typical of the White Bark shear zones (Fig. 3b). Gradational margins, where strain increases continuously albeit steeply, from the host-rock into the structure are the exception for these sheared aplite dikes (Fig. 4).

Along the SSZ, lineations are developed both in the plane of the mylonitic foliation and locally in adjacent wall rocks, especially where a broader strain gradient defines the zone margin. Lineations are composed of elongate aggregates of fine-grained mylonite. In gradational margins, a lineation is defined by elongate and smeared biotite grains. Lineations along the SSZ show a fairly uniform orientation, raking 7°–12°W (Figs 5 & 6).

Figure 5 shows an interpreted cross-sectional view of the NSZ and SSZ looking north, approximately perpendicular to the plane of the shear zones. The net offset vector, computed from three-point problems on crossing dike pairs, is shown by the heavy arrow at point E. The tip-line of the SSZ at high angles to the net offset vector is visible in the central part of the section at point A; the upper tip-line, at low angles to the net offset vector, is upslope to the east at point B. Older markers within the host granite—such as crossing aplite or pegmatite dikes, bands of alkali-feldspar megacrysts, mafic inclusions and mafic schlieren—record the amount of offset along the shear zones (barbed arrows). We use the term 'offset' here to refer to the tangential separation of crossing markers (i.e. within the plane of Fig. 5). This is roughly analogous to the discontinuity in the displacement field for faults modeled as shearing cracks in continuum mechanics (Bürgmann et al., 1994), although there is generally not a single material surface across which sliding occurs. In the case of these shear zones, the displacement field may not contain a discontinuity. Rather, considering a reference frame with two co-ordinates in the plane of the shear zone and the origin at the shear-zone center, the displacement field would be continuous but change sign over a tabular volume of finite width. Crossing aplite dikes are particularly useful offset markers as they are well defined and are roughly planar. Some dikes depart from an ideal tabular geometry, imparting an uncertainty to the offset estimate.

At one point, a single continuous dike shows a gradually curving trace (near point C, Fig. 2). Along the central portion of the dike, roughly parallel to the NSZ and SSZ, a streaky mylonitic fabric parallels the dike margins, the dike is finer grained, and crossing markers are offset by up to 2 cm. Portions of the dike that are at high angles to the main shear zones show no mylonitic fabric and no offset of cross-cutting markers.

For the most part, offset dikes are subvertical and essentially parallel, making it difficult to determine the true direction of net offset. However, at the western end of the White Bark outcrop (Fig. 2, point E), two aplite dikes strike NW, counter to the usual NE strike. The locations of several points along these crossing dikes were surveyed in order to determine the three-dimensional orientation of the dikes and the NSZ. From these orientations, the intersection line between the NW-striking dikes and the NE-striking dikes allows calculation of the net offset vector which is 0.75 m in magnitude and rakes 15°W (see heavy arrow in Fig. 5 and filled square in Fig. 6).

The incremental offset direction, recorded by lineations, is essentially parallel to the net offset vector, as determined by crossing dikes. Because the outcrop surface is approximately perpendicular to the offset dikes (subvertical), the apparent offset of crossing aplite dikes closely approximates the true offset. Offset of crossing markers is left-lateral and varies in magnitude from <1 to 700 cm.

Fig. 2. Geological map of 'White Bark' outcrop. The upper part of the map is continuous with the lower. Shear zones shown in heavy lines, offset dikes as a dashed line and younger fractures shown with a gray line. Dotted lines are topographical contours with approximate elevation in meters. The shaded area is covered. Original mapping done at 1:200 scale using 219 control points whose locations were surveyed using an electronic theodolite and electronic distance meter (EDM). Control locations were reproducible to <5 cm which is approximately equivalent to the line width on the original map. Mapping was then completed by numerous measurements using a compass and tape measure.
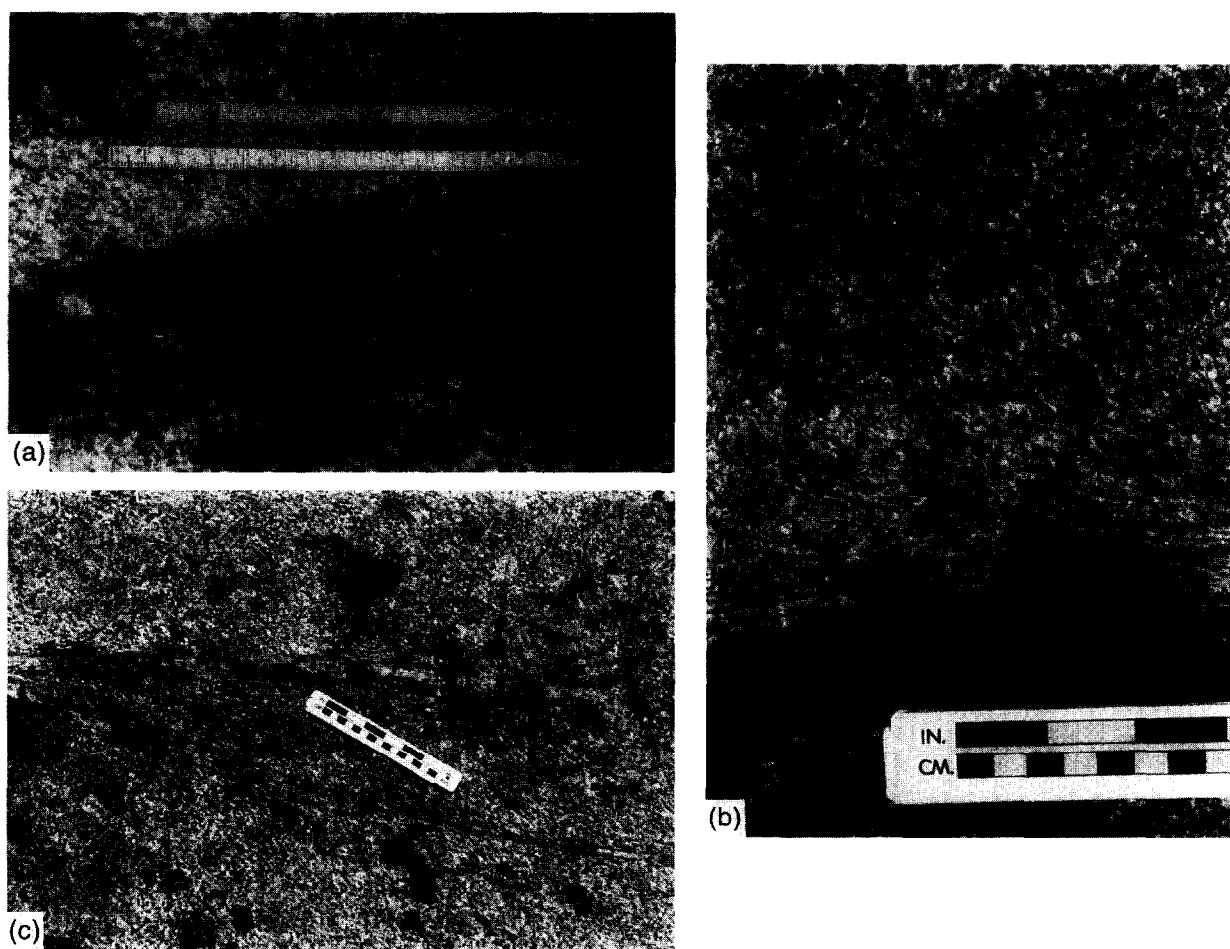
Fig. 3. Photographs showing aspects of shear-zone structures. (a) Sharp boundary typical of most shear-zone margins; (b) gradational margin from near point D, Fig. 2. See text for discussion. (c) Photograph of a fork in the NSZ (Fig. 2). Note the preservation of the original aplite dike near the upper edge of the photograph. Sheared aplite extends constitutes the fork in the right-hand part of the photograph. To the right, a shear zone is developed in the host-rock granite, rather than being confined to the aplite.

The distribution of width and offset as a function of position along the shear-zone trace for the NSZ and SSZ is plotted in Fig. 7. The distributions show lesser values near the lateral tips of the shear zone and greater values near the center. Large offset values along the central portion of the structure are generally associated with a greater shear-zone width, suggesting that the shear zones grew in width as they accumulated offset. At the western end of the SSZ (point A, Fig. 2), a vertical, opening-mode fracture emanates from the tip of the shear zone and extends at an azimuth of 065° for about 4 m into the extensional (south-west) quadrant of the shear zone. The fracture tapers from 6 cm in width, where it is filled by vein quartz, to a hairline crack.

We interpret this fracture as a 'splay crack', analogous to the secondary fractures that form at the tips of shear-mode fractures in laboratory fracture experiments (Erdogan and Sih, 1963; Ingraffea, 1981) and to cracks at the tips and at steps in small faults (Segall and Pollard, 1983; Martel et al., 1988). The orientation of the splay crack is consistent with the relative motion on the SSZ being left-lateral and strike-slip.

The larger shear zones are not simple, continuous structures but rather are composed of several approximately co-planar segments. Segments along the NSZ average ∼5 m in length and are arranged in a right-stepping, en échelon geometry. At steps between segments, the shear zone appears to fork (Figs 2 & 3c), and shear on one fork decreases gradually as shear is transferred to the opposing fork. Within the step-over region, shear may be transferred through granite host-rock rather than aplite.

In contrast, the SSZ appears at map scale to be less segmented and more continuous (Fig. 2). East of point D, for some 20 m, the shear zone consists of two subparallel strands separated by 1.5–2 m of relatively undeformed granite. Within this region of otherwise undeformed granite, a small left-lateral shear zone connects the main shear-zone strands (Fig. 2, point D). In other places, especially along the SSZ, similar subparallel segments are also found at a smaller scale .where the segments are separated by 1–5 cm wide septa of relatively undeformed host-rock.
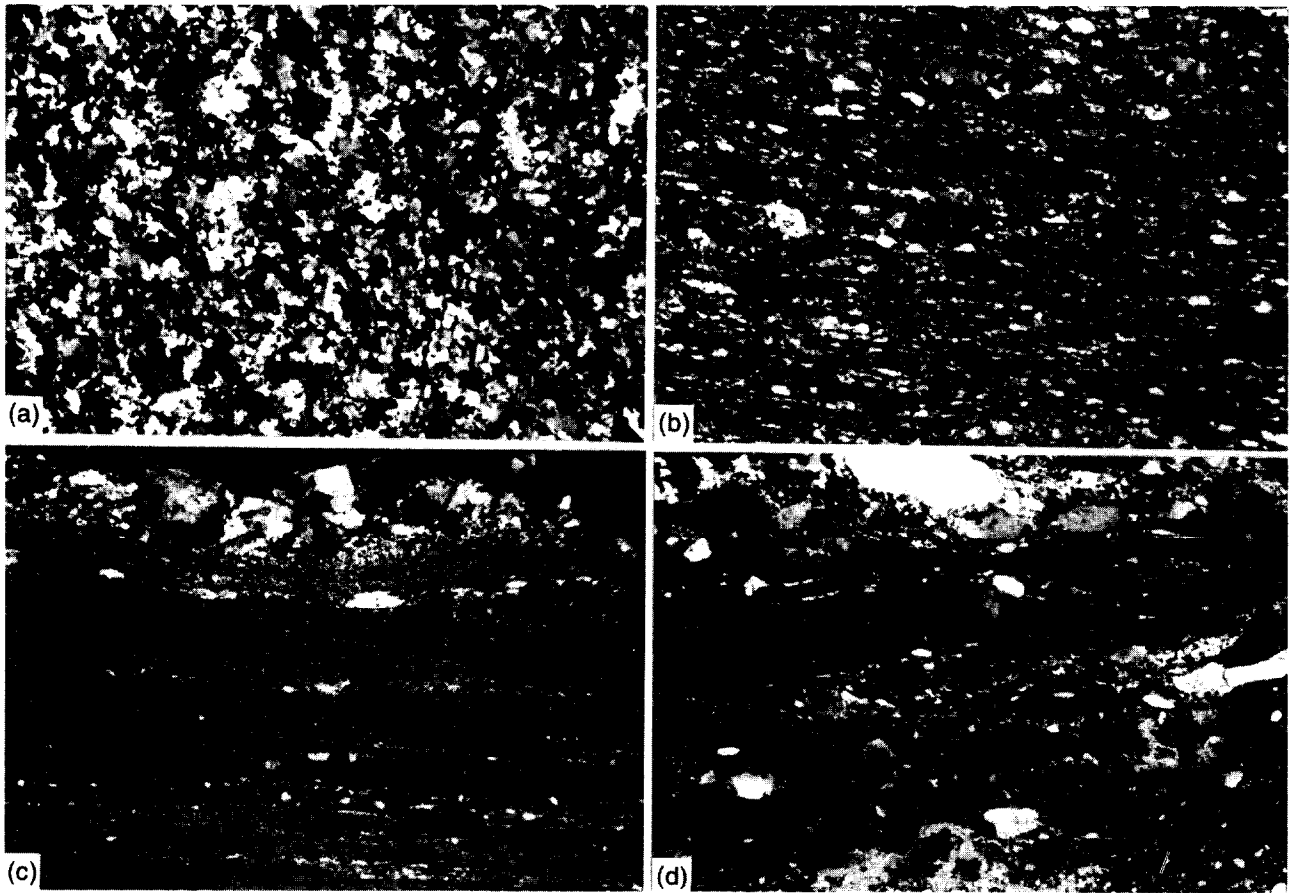
Fig. 4. Photomicrographs showing fabric development with progressive shear of aplite dikes. The field of view in all cases is approximately 1.1 × 1.5 mm. (a) Sample PHB93.2 from unsheared dike. (b) Sample PHB93.5, shear strain 3.6–5.0, shows the beginning of a mylonitic foliation and grain-size reduction. (c) Sample PHB91.1, shear strain 37.8–39.2, shows a substantial grain-size reduction. The upper part of the photograph shows a sharp contact with wall-rock granite. (d) An example where feldspar porphyroclasts are relatively coarse and occur in a very fine matrix of quartz. Sample PHB93.11, shear strain 65.3–66.9. The upper part shows the contact with the wall-rock granite.
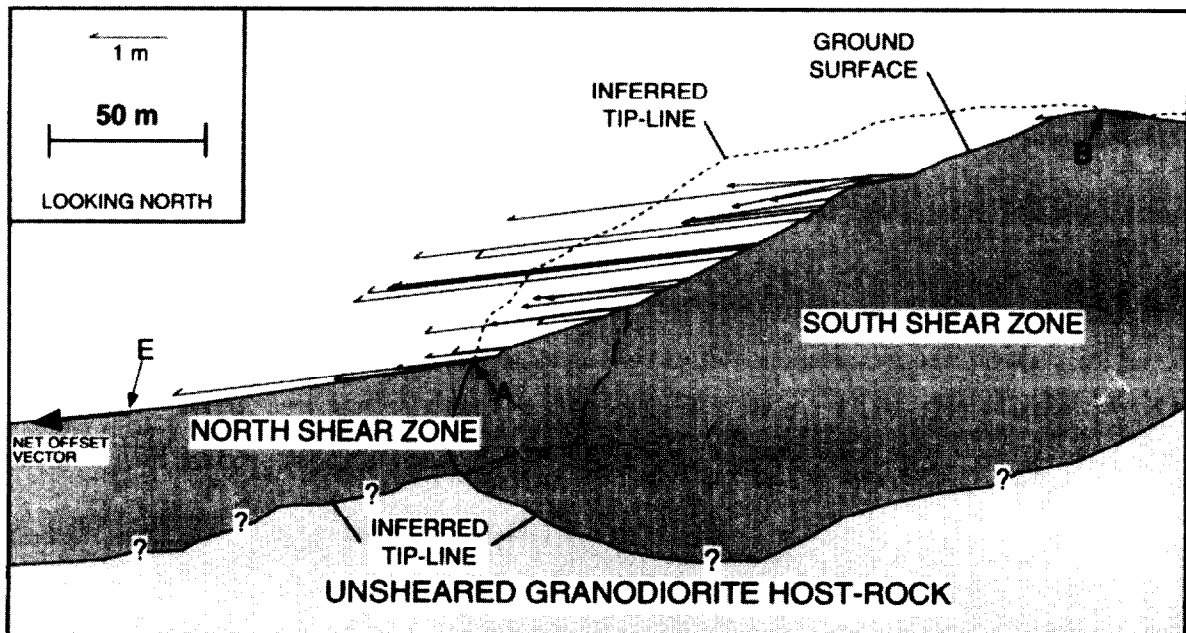

Fig. 5. Cross-section of the NSZ and SSZ looking approximately normal to the structures. Small arrows with triangular heads show the projection of measured lineations (arbitrary magnitude). Barbed arrows show the apparent offset of crossing aplite dikes, assumed to be parallel to lineations (see magnitude scale, upper left). Heavy arrow at the western edge of the cross-section shows computed net offset vector, as described in the text and shown in Fig. 6. Points A, B and E coincide with same points in Fig. 2.
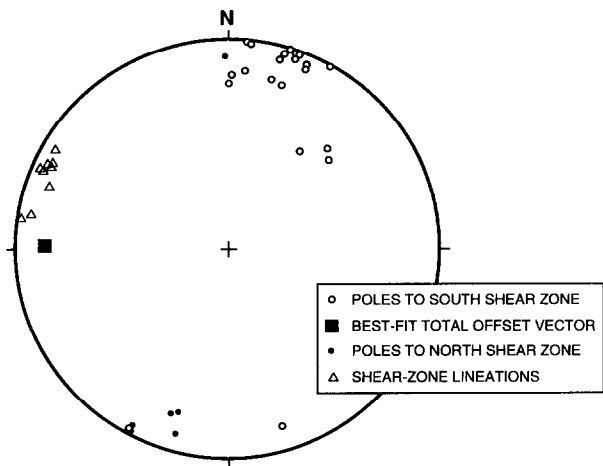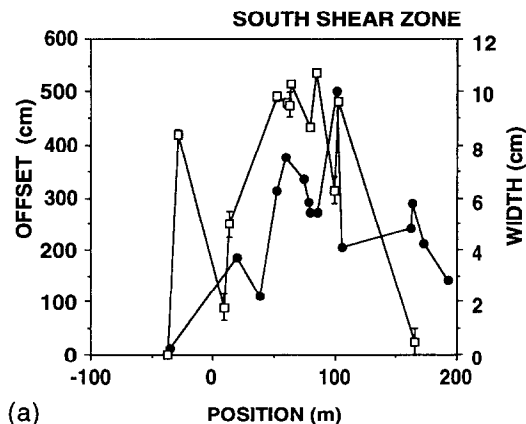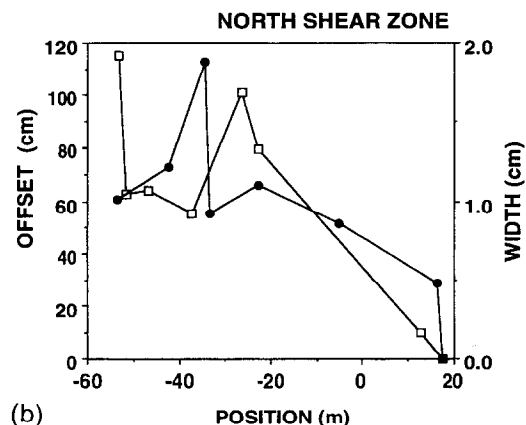
Fig. 6. Lower-hemisphere equal-area plot of structural elements of the NSZ and SSZ (Fig. 2). Open circles show poles to segments of the SSZ; filled circles are poles to segments of the NSZ; triangles are lineations. The filled square shows the net offset vector determined by three-point solutions for the NSZ (see text).

(a)

(b)

Fig. 7. Offset and width vs position for the NSZ and SSZ. Offset plotted in open boxes, width in black circles (both in cm). Note the different scales on each plot. A unique uncertainty is assigned for each offset measurement assuming that, where well exposed, offset can be measured to ± 1 cm. Where dikes are projected under cover, over distances < 1 m, locations can be extrapolated to ± 5 cm; where projected over distances > 5 m, locations can be extrapolated to ± 25 cm. The measured width is the sum of the widths at a given locality if subparallel shear-zone segments exit. The value excludes the width of any undeformed host-rock (septa) between the segments.

SHEAR STRAIN ESTIMATES

Crossing dikes were used to estimate the shear-zone accommodated offset at several points along the shear zones. Offset divided by the shear-zone width provides an estimate of the average shear strain (γ) represented by the shear zones. These shear strain estimates represent upper bounds as the true strain may be less than the determined value if there is sliding across material discontinities. However, there is no evidence for discrete slip, even at the microscopic scale (see below). We focus here on strain estimates made at the location of microstructural samples (described in the next section). The resulting values show a range of 3 orders of magnitude in shear strain. Uncertainty in the strain estimate comes primarily from the uncertainty in estimating the offset (see Fig. 7). Some attempt was made to sample the shear zones as near to offset markers as possible. Away from offset dikes, offset along the shear zones is estimated by averaging that determined from the two nearest dikes; this interpolation contributes an additional unknown uncertainty to the strain determination which is not included in the reported value. The locations of the microstructural samples are shown in Fig. 2. Because of this, the location of sample sites used in estimating shear strain relative to offset markers is important. We therefore describe the sample localities in some detail. Sample localities are shown in Fig. 2.

Samples PHB93.2–PHB93.7 come from the curving sheared dike at point C (Fig. 2). Although samples along the curving dike show relatively low strain, the structure represents clear evidence for the importance of dike orientation in resolving shear stress. Along the more N-striking segments, bands of alkali-feldspar megacrysts and mafic schlieren show no offset where they cross the curving dike. This constrains the shear strain to be essentially zero in the vicinity of samples PHB93.2 and PHB93.7. In the central portion of the sheared dike, a crossing aplite dike 45 cm along the shear zone to the east of sample PHB93.5 and 70 cm west of sample PHB93.4 shows 6.0 cm of left-lateral offset. A distinctive zone of mafic minerals adjacent to a collection of feldspar megacrysts is left-laterally offset by 1.2 cm at a location 107 cm west along the sheared dike from sample PHB93.5. Ten centimeters away from sample PHB93.3 a crossing dike shows an apparent left-lateral offset of 9.0 cm. However, the irregular shape of the crossing dike makes for some uncertainty in the offset measurement.

Samples PHB93.8–PHB93.11 were collected from along the NSZ and generally represent intermediate values of shear strain. Sample PHB93.8 was collected 440 cm east of a pegmatite dike that is left-laterally offset by 63.9 cm. Two additional left-lateral offset measurements of 57.5 and 66.5 cm from within the mafic enclave shown near the west end of Fig. 2 support this offset estimate. Sample PHB93.9 lies 127 cm east of a crossing dike that is offset by 55.2 cm. Exposure of the dike along

Table 1. Measured shear strain and grain size for selected samples (in order of increasing shear strain)

Sample	Shear zone	Width (cm)	Offset (cm)	Average shear strain*	Average grain size (μm)
PHB93.2	CSZ	5	0.0±1.0	0.1±0.1	229.5
PHB93.7	CSZ	2.7	0.0±1.0	0.1±0.1	
PHB93.6	CSZ	2.8	1.2±1.0	0.4±0.4	129.5
PHB93.16	SSZ	4.8	25.0±25.0	2.6±2.6	
PHB93.4	CSZ	1.8	5.4±1.0	3.0±0.6	88.1
PHB93.17	SSZ	4.2	25.0±25.0	3.0±3.0	
PHB93.3	CSZ	2.2	9.0±1.0	4.1±0.5	
PHB93.5	CSZ	1.4	6.0±1.0	4.3±0.7	72.6
PHB93.8	NSZ	2.3	63.9±1.0	27.8±0.4	61.6
PHB93.9	NSZ	1.9	55.2±1.0	29.1±0.5	82.1
					56.8†
PHB91.1	SSZ	12.5	480.9±9.1	38.5±0.7	
PHB93.10	NSZ	1.8	79.4±1.0	44.1±0.6	
PHB93.13	SSZ	6.0‡	361.9±25.0	60.3±4.2	
PHB93.11	NSZ	1.2	79.3±1.0	66.1±0.8	
PHB93.12	SSZ	5.0‡	352.5±5.0	70.5±1.0	
PHB91.2	SSZ	6	432.8±10.8	72.1±1.9	
PHB93.15	SSZ	2.8	236.0±1.0	84.3±0.4	
PHB93.14	SSZ	4.7	490.6±8.2	104.4±1.75	

*Uncertainty in offset is estimated as in Fig. 7; where sample is between offset dikes, offset measurements are averaged.
†Two grain-size samples were taken in different regions of the specimen (see Fig. 4d).
‡Because of incomplete exposure, width is a minimum.

strike shows that it is steeply dipping. Sample PHB93.11 was collected 700 cm east of the 55.2 cm offset measurement, and 300 cm west of a dike offset by 101 cm. Sample PHB93.10 lies 140 cm east of a dike left-laterally offset by 79.4 cm.

The remaining samples (PHB93.12–PHB93.17) come from the SSZ and generally represent the largest strain magnitudes. Although only 660 cm from the tip-line of the SSZ, sample PHB93.12 lies 200 cm west (toward the tip-line) of a crossing aplite dike that is offset by 352.5 cm, suggesting a very steep strain gradient along strike. There is, however, some curvature in the crossing dike which makes determination of the offset somewhat difficult. Offset in the vicinity of sample PHB93.13 is one of the least well-constrained of the samples in Table 1. The sample was collected about 16 m west of a dike showing 491 cm of left-lateral offset and 20 m east of a well-exposed dike showing 232.8 cm of offset. The locality of sample PHB93.14 is coincident with the intersection of the western segment of the SSZ and the dike offset by 491 cm (Fig. 2).

Samples PHB91.2 and PHB93.15 are from within a large (~20 m long) fork in the SSZ (Fig. 2). Sample PHB91.2 was collected from the intersection of the southern fork of the SSZ and the crossing shear zone mentioned earlier. Two subvertical aplite dikes are offset by this forked portion of the SSZ for a total offset (summing both of the forked segments) of ~5 m. The western dike is offset by 138 cm on the northern fork and 294 cm on the southern fork. Although sample PHB91.2 was collected from the southern fork, because it lies very near the tip-line of the northern segment, we infer that the total offset of 432.8 cm across both forks best approximates the offset accommodated by the SSZ at the locality

of the sample. Sample PHB93.15 was collected from between the two offset dikes along the northern fork. The dike 320 cm to the west of the sample locality is offset by 138 cm and the dike 130 cm to the east is offset by 334 cm.

Sample PHB92.3 was collected from a small outcrop within a covered area along the NSZ. An offset segment of a crossing aplite dike lies within the septum between two forked strands of the NSZ, 205 cm to the east along strike. The continuation of the dike to the north is covered, making determination of the offset on the north side difficult. To the south, however, the same dike is left-laterally offset by 314 cm. A second dike, essentially coincident with the sample locality, is offset by 481 cm. Sample PHB93.1 was collected 12.6 m to the east along strike of the NSZ. No other dikes were observed, other than those in the vicinity of PHB92.3.

Samples PHB93.16 and PHB93.17 are from the less well-exposed easternmost extent of the NSZ. Only one offset dike was observed in this area, lying 350 cm east of sample PHB93.16 and about 11.5 m west of PHB93.17. The dike is left-laterally offset by 25 cm. The quality of this determination is relatively poor due to projecting the dike under about 2.5 m of cover to the south of the NSZ and under about 9 m of cover to the north.

MICROSTRUCTURE

The Mono Creek Granite has a typical seriate, hypidiomorphic-granular texture with grains that range in size from 125 μm to several cm. Coarse alkali-feldspar phenocrysts are conspicuous in the field and are commonly ~2.5 cm in length, whereas groundmass quartz is typically ~1–2 mm. Plagioclase and alkali-

feldspar grains in the host-rock are interlocked on a fine scale. Aplite dikes are much finer grained (0.1–1.2 mm) and show an equigranular, phaneritic texture. Instead of being interlocked, feldspar grains are equant and tend to abut one another as well as abutting comparably sized quartz grains.

In order to investigate how the shear zones evolved microscopically, we collected several samples from shear zones at various stages of development (Fig. 2). Average shear strain (γ) is determined by measuring the offset of aplite dikes and dividing by the shear-zone width (Table 1).

The first observed change in deformed aplite dikes is the appearance of a foliation in samples that have experienced shear strain of $\gamma \sim 3.5$–5.0 (Fig. 4a). This foliation is oriented roughly parallel to the shear-zone margin and is defined by aligned aggregates of fine-grained quartz that surround feldspar porphyroclasts, and by the arrangement of mineral grains into rows separated by thin (8–20 μm) quartz-filled seams that cut across grains. Elongate quartz grains within the seams define a grain-shape foliation that is oriented at moderate angles to the main foliation. The orientation of this grain-shape foliation is consistent with the overall sense of shear inferred from offset markers. Interference colors for these grains indicate a lattice-preferred orientation, suggesting that they form by recrystallization during shear deformation. Near the edges of sheared aplite dikes, host-rock micas may show a strong alignment and probably helped to localize shearing.

For shear strains of $\gamma \sim 5$, quartz and feldspar grains are diminished substantially in size (average grain size reduces from 230 to $\sim 70\, \mu$m) and have a strong alignment (Fig. 4b). This grain-size diminution imparts a black color to the mylonite at the hand-sample scale. Observing the textures at progressively higher strain, feldspar porphyroclasts appear to be pulled apart into trails of finer grains (Fig. 4c). This takes place by fracturing of the grains along cleavage planes and the progressive rotation and translation of the grain fragments as shear continues. However, deformation of feldspar is not limited to fracturing. The upper part of the photograph shows a typical, sharp contact with the wall-rock granite. Although the contact is sharp, there is enough relief on the surface to preclude discrete sliding at the shear-zone boundary. (The photograph is taken perpendicular to foliation and parallel with lineation.) This absence of discrete surfaces across which sliding might have occurred is characterstic of the shear zones.

At higher strain ($\gamma \sim 30$), feldspar porphyroclasts show bent cleavage and undulose extinction, suggesting that feldspar deforms in part by crystal–plastic deformation mechanisms. For shear strain $\gamma > 50$, grain size is very fine (average grain size is 60–80 μm) and the foliation is well developed (Fig. 4d). Note the finer grain size in the matrix of Fig. 4(d) compared to Fig. 4(c), yet the relatively coarse porphyroclasts in the higher-strain sample. Portions of the shear zone that show larger porphyroclasts

probably reflect incorporation of wall-rock granite in addition to aplite.

In order to investigate the relation between grain size and shear strain in the mylonite, we measured the grain size using a petrographic microscope on thin sections oriented perpendicular to the shear-zone margins and approximately parallel with the offset direction. In order to limit measurement biases, measurements were made along regular traverses across the thin section, approximately perpendicular to foliation. The microscope stage was advanced by a regular interval using a mechanical point-counting stage, and the apparent grain diameter was measured using a graduated cross-hair. Measurement was not always made on the center-line of the grain, but we assume that given a sufficient sample size ($N = 100$), variations in the apparent diameter caused by measuring away from the center-line are averaged out. Grain-size results are reported in Table 1 and Fig. 8.

The mean grain size of undeformed aplite is $\sim 230\, \mu$m. As the dikes begin to shear, this value decreases sharply to 70–90 μm at $\gamma \sim 5$, then remains approximately constant as strain increases (Fig. 8a). The undeformed aplite sample shows a slightly skewed grain-size distribution (Fig. 8b). As shear strain increases, the skewness increases slightly and the mean size decreases, but the maximum size stays relatively constant (Fig. 8c–e). As γ reaches ~ 30, the porphyroclast size also begins to decrease, reflected in a decrease in skewness (Fig. 8f–g).

In most of the samples investigated, the grain-size distribution and texture is relatively uniform over the scale of the thin section (several cm). Occasionally, however, the texture is distinctly non-uniform (e.g. sample PHB93.11, Fig. 4d), consisting of subdomains where the matrix grain size is much finer. Porphyroclasts in these samples remain much coarser than is typical for similar samples at comparable strain. (See also sample PHB93.9, Table 1.) As mentioned above, this probably reflects incorporation of wall-rock granite into the shear zone.

Occasionally, vein-like fractures are found oriented parallel to the shear zone and filled with elongate quartz grains showing recrystallization textures. In thin section, the quartz grains define a grain-shape foliation that is inclined with respect to the main mylonitic foliation. Again, this foliation is consistent with the overall sense of shear. Quartz shows a strong preferred crystallographic orientation and abundant subgrains (portions of the grain with the crystal lattice oriented mis-aligned by a few degrees). The quartz grain shape and character are consistent with the vein-like fractures having formed under a combination of opening and shear, although the shear strain may be of a lesser magnitude than that in the surrounding mylonite.

DISCUSSION
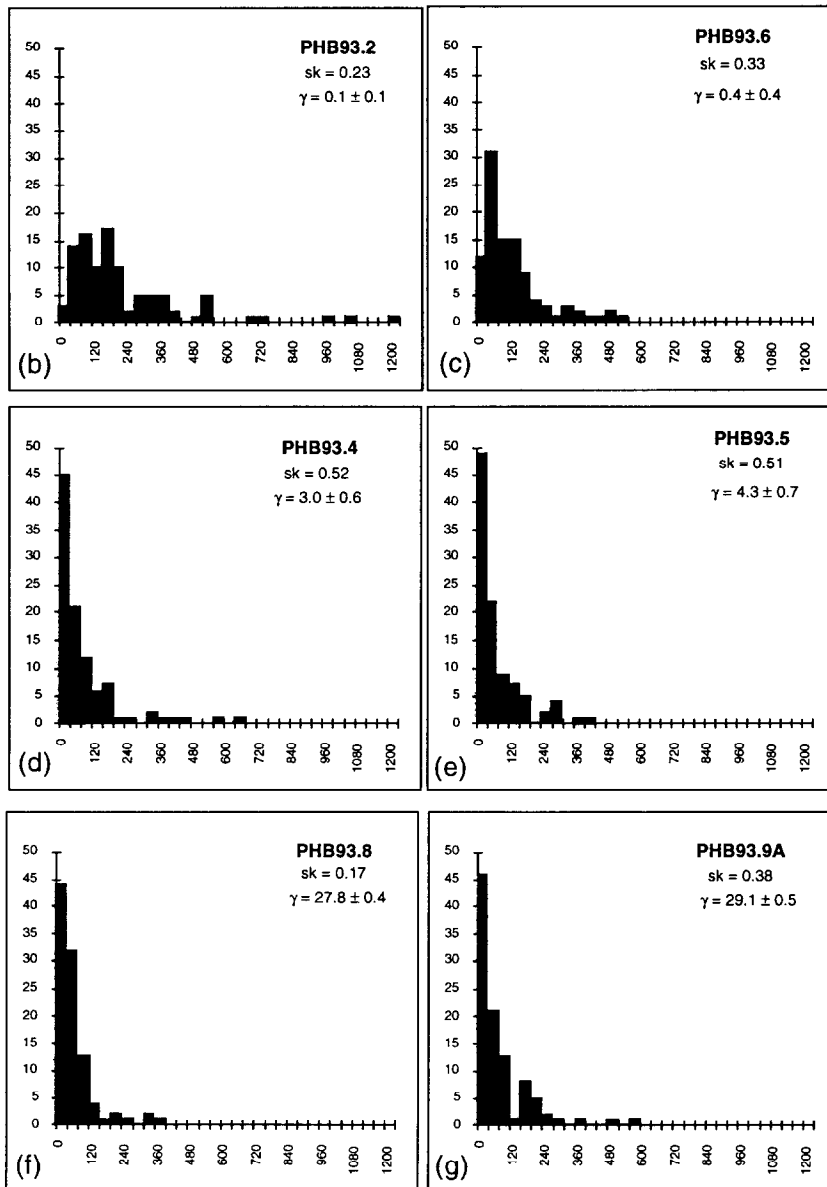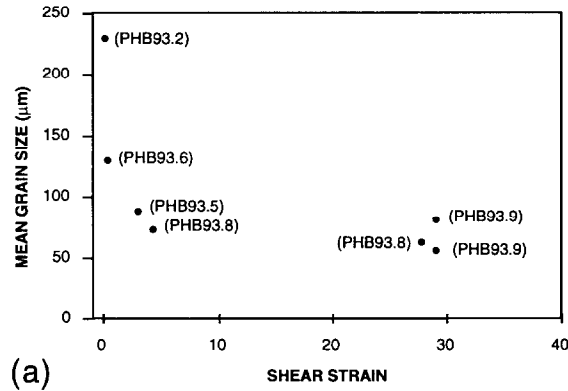
Following crystallization of the Mono Creek Granite,

Fig. 8. Grain-size data for samples described in the text. (a) Mean grain size falls off sharply as shear strain increases then retains a relatively constant value of ~75 μm. (b–g) Frequency distribution of grain size (μm) for selected samples representing a range of shear strain. 'sk' is the skewness as given by sk = (upper quartile + lower quartile − 2 × median)/interquartile range. (b) Sample PHB93.2 is from an unsheared aplite dike. The remaining samples are from shear zones at various stages of development and therefore various shear strains (see Table 1).

the last phases of magmatic activity involved the emplacement of a series of aplite and pegmatite dikes in various orientations. An orientation subset of these aplite dikes was sheared to form mylonitic shear zones. Several lines of evidence lead us to interpret the different mylonitic shear zones exposed in this region as representing members of an evolutionary sequence of progressively sheared aplite dikes:

(1) preservation of aplite dikes with various degrees of mylonitic fabric development;

(2) correlation between the development of the mylonitic fabric and the apparent offset of crossing markers;

(3) preservation of decimeter-scale irregularities such as forks, jogs, bends and septa in the shear zones that are geometrically similar to such irregularities in nearby aplite dikes; and

(4) correlation between the orientation of a continuous, curved aplite dike (point C, Fig. 2), the occurrence of mylonitic fabric and offset of crossing markers.

We hypothesize that the *fine grain size* and *textural characteristics* of the aplite lithology were critical in providing zones of weakness that localized shear deformation. In cases where subparallel aplite and pegmatite dikes occur, the aplites show the development of mylonitic fabrics whereas the pegmatite dikes do not. Because feldspar dominates the strength of granitic rocks at greenschist-facies conditions, the arrangement of feldspar grains plays a crucial role in the overall deformation behavior of quartzo-feldspathic aggregates (Jordan, 1988; Tullis, 1990). In addition to being finer grained, aplites have a relatively uniform distribution of equant quartz and feldspar grains (allotriomorphic granular texture), presumably because of the crystallization of aplite near the peak rate of crystal nucleation (Cox et al., 1979). We infer that the relatively fine grain size and equant character of feldspar and the general lack of interlocking textures makes the aplite dikes significantly weaker than the surrounding granite, causing shear strain to be localized along the dikes.

We further hypothesize that the *orientation* of dikes with respect to the remote stress field was a critical parameter in the formation of these structures. Only subvertical aplite dikes oriented $090° \pm 20°$ are observed to localize left-lateral shear strain. We interpret the opening fracture at the western tip of the South shear zone (near point A, Fig. 2) as being analogous to the opening cracks that are developed at the tips of small faults elsewhere in this region (Segall and Pollard, 1983; Martel et al., 1988). If this interpretation is correct, it constrains the orientation of the maximum compression to be approximately in the horizontal plane and at $30° \pm 5°$ counter-clockwise to the shear zone during deformation. Apparently this was the orientation of principal stresses in the remote field that resolved the critical tractions on the aplite dikes to initiate shearing.

The critical orientation of the parent dike is especially evident where a single curving dike varies gradually and continuously from being at a high angle to the well-developed shear zones to being essentially parallel to the zones (near point C, Fig. 2), and only that portion of the dike roughly parallel to the shear zones has accumulated shear strain.

Shear-zone growth

Detailed observations at the White Bark outcrop suggests that geometric irregularities in the trace of the shear zones, including forks, eyes, jogs and septa (Fig. 3c), are partly inherited from the irregular initial arrangement of the parent dikes. Vestiges of the aplite dikes are especially well-preserved along the NSZ (Fig. 2) where average strain is lower and the mylonitic fabric is less intense. Forks in the zone, tens of centimeters in size, form where discontinuous dike segments in an en échelon geometry merge into a through-going shear zone. Along one branch of the fork, intact aplite-dike material is preserved while the other has been intensely mylonitized (Fig. 3c). Where the strain is greater, the forks are larger, reaching tens of meters in length (point D, Fig. 2). In these cases, remnants of the original dike material apparently were obliterated by the deformation.

From the field relations, we infer that forks in the shear zones form as originally discontinuous aplite dikes localize sufficient shear to link together (Fig. 9). With continued shear, both strands of the shear zone accommodate some of the shear strain, resulting in a shear zone with a branching trace. If a through-going shear zone is established, a greater net offset may be accumulated and decimeter-scale irregularities, such as septa of undeformed wall-rock, are obliterated as they are incorporated into the zone. Parts of a shear zone with greater offset magnitudes were able to link to more widely spaced initial dikes, leading to larger irregularities in the resulting shear zone. This mechanism for shear-zone growth by end-to-end linkage of segments contrasts with continuous in-plane propagation from a single tip line (Ramsay, 1980). This also contrasts with the way in which some faults propagate by end-to-end linkage of shearing surfaces by opening-mode fractures (Segall and Pollard, 1983; Martel et al., 1988). The different character of the NSZ and the SSZ probably results from differences in: (1) the initial arrangement of dike segments that linked by shearing to produce the shear zones; (2) a difference in the net offset magnitude on each structure; and (3) the slightly different orientation of the shear zones with respect to the applied stress field during deformation.

Shear-zone width shows a positive correlation with shear offset (Fig. 7), suggesting that, in addition to growing in length, the shear zones grew in width as they accumulated shear. Growth in width may take place via two different mechanisms: (1) by the progressive incorporation of wall-rock mineral grains into the shear zone;
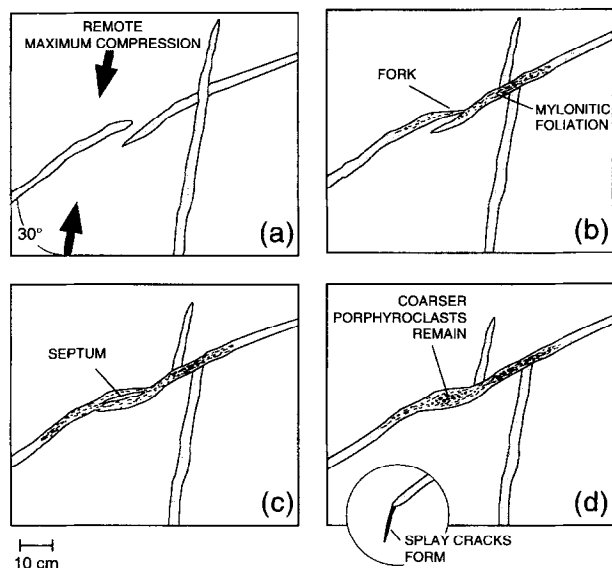
Fig. 9. Schematic structural evolution of shear zones. (a) Arrangement of crossing dikes prior to shear. Plausible orientation of maximum compression is also shown. Note that the older dike is discontinuous, showing an left-stepping en échelon geometry similar to that seen on the NSZ, Fig. 2. (b) As dikes with a high resolved shear stress begin to shear, a mylonitic fabric develops (shown schematically with short tics). With continued shear, the shear zone propagates in its own plane or curves slightly as it interacts the neighboring shear-zone segment, producing a fork, such as that shown in Fig. 3(c). Note offset of crossing dike has increased. (c) As shear continues, the opposing fork develops, isolating a septum of undeformed host rock. (d) At higher strain, these septa begin to deform and produce regions of relatively coarse porphyroclasts similar to that shown in Fig. 4(d). Eventually, splay cracks may propagate from the tip of the shear zone. See text for further discussion.

or (2) by the side-to-side merging of subparallel segments. We infer that the later process is largely responsible for the observed irregularity of the shear-zone width along strike (Fig. 7). Significant growth in width may require the presence of pre-existing subparallel dikes which appear to have progressively merged together to varying degrees: in some cases 'septa' of less deformed host-rock granite remain between subparallel strands of the shear zones; elsewhere, eye-shaped inliers of granite are found; occasionally only regions of unusually coarse porphyroclasts are all that remain (Fig. 9). We interpret these relationships to show that the shear zones grew in width by the progressive incorporation of coarser-grained (and probably stiffer) wall-rock granite. Growth in width was probably enhanced where subparallel aplite dikes existed prior to shearing.

Theoretical studies of the origin of shear zones commonly appeal to instabilities related to the rheological laws of the deforming materials as a means of localizing shear strain. While shear instability in either the brittle regime (Rudnicki and Rice, 1975) or the ductile regime (Poirier, 1980) is undoubtedly important, in a heterogeneous crust shear of inherently weak zones is also a viable means of localizing shear strain and thus a plausible explanation for the origin of, at least, some shear zones. One example where this has been demonstrated is the material heterogeneity associated with chemical weakening by water-rich fluids along discrete

fractures (Segall and Simpson, 1986; Kronenberg et al., 1990). In this study, we discuss another example where shearing apparently is localized by differences in rock type. The tabular aplite dikes apparently were weaker because of finer grain size and because feldspar grains tended to abut one another whereas in the host granite they are interlocked.

REFERENCES

Ague, J. J. and Brimhall, G. H. (1988) Magmatic arc asymmetry and distribution of anomalous plutonic belts in the batholiths of California. Bulletin of the Geological Society of America 100, 912–927.
Bateman, P. C. (1992) Plutonism in the Central Part of the Sierra Nevada Batholith, California. U.S. Geological Survey Professional Paper 1483.
Bateman, P. C., Clark, L. D., Huber, N. K., Moore, J. G. and Rinehart, C. D. (1963) The Sierra Nevada batholith—a synthesis of recent work across the central part. U.S. Geological Survey Professional Paper 414D, D1–D46.
Beach, A. (1980) Retrogressive metamorphic processes in shear zones with special reference to the Lewisian complex. Journal of Structural Geology 2, 257–263.
Bonafede, M. (1990) Anelastic processes and stress transfer from shallow to deep fault regions. Tectonophysics 182, 1–7.
Brace, W. F. and Byerlee, J. D. (1970) California earthquakes: why only shallow focus? Science 168, 1573–1575.
Bürgmann, R., Pollard, D. D. and Martel, S. J. (1994) Slip distributions on faults: effects of stress gradients, inelastic deformation, heterogeneous host-rock stiffness, and fault interaction. Journal of Structural Geology 16, 1675–1690.
Byerlee, J. D. (1968) Brittle–ductile transition in rocks. Journal of Geophysical Research 73, 4741–4750.
Christiansen, P. P. (1995) Faulting and hydrothermal processes in a granitic batholith. Ph.D. thesis, Stanford University.
Cohen, S. C. (1981) Postseismic rebound due to creep of the lower lithosphere and asthenosphere. Geophysical Research Letters 8, 493–496.
Coward, M. P. (1976) Strain within ductile shear zones. Tectonophysics 34, 181–197.
Coward, M. P. and Potts, G. J. (1983) Complex strain patterns at the frontal and lateral tips to shear zones and thrust zones. Journal of Structural Geology 5, 383–399.
Cox, K. G., Bell, J. D. and Pankhurst, R. J. (1979) The Interpretation of Igneous Rocks. George Allen and Unwin, London.
Dragoni, M., Bonafede, M. and Boschi, E. (1986) Shallow earthquakes in a viscoelastic shear zone with depth-dependent friction and rheology. The Geophysical Journal of the Royal Astronomical Society 86, 617–633.
Dragoni, M. and Pondrelli, S. (1991) Depth of the brittle–ductile transition in a transcurrent boundary zone. Pure and Applied Geophysics 135, 447–461.
Erdogan, F. and Sih, G. C. (1963) On the crack extension in plates under in plane loading and transverse shear. ASME Journal of Basic Engineering 85, 519–527.
Everden, J. F. and Kistler, R. W. (1970) Chronology of Emplacement of Mesozoic Batholithic Complexes in California and Western Nevada. U.S. Geological Survey Professional Paper 623.
Hobbs, B. E., Ord, A. and Teyssier, C. (1986) Earthquakes in the ductile regime? Pure and Applied Geophysics 124, 309–336.
Huber, N. K. (1981) Amount and Timing of Late Cenozoic Uplift and Tilt of the Central Sierra Nevada, California—Evidence From the Upper San Joaquin River Basin. U.S. Geological Survey Professional Paper 1197.
Ingraffea, A. R. (1981) Mixed-mode fracture initiation in Indiana

Limestone and Westerly Granite. In *Proceedings of the 22nd Symposium on Rock Mechanics*, pp. 186–191.

Jordan, P. (1988) The rheology of polymineralic rocks—an approach. *Geologische Rundschau* **77**, 285–294.

Kirby, S. H. (1985) Rock mechanics observations pertinent to the rheology of the continental lithosphere and the localization of strain along shear zones. *Tectonophysics* **119**, 1–27.

Kronenberg, A. K., Segall, P. and Wolf, G. H. (1990) Hydrolytic weakening and penetrative deformation within a natural shear zone. In *The Brittle–Ductile Transition—The Heard Volume*, ed. A. G. Duba, pp. 21–36. American Geophysical Union, Geophysical Monograph **56**.

Lachenbruch, A. and Sass, J. (1973) Thermo-mechanical aspects of the San Andreas. In *Proceedings of the Conference on the Tectonic Problems of the San Andreas Fault System*, eds R. Kovach and A. Nur, pp. 192–120. Stanford University Publications in the Geological Sciences **13**.

Lockwood, J. P. (1975) *Mount Abbot Quadrangle, Central Sierra Nevada, California—Analytic Data*. U.S. Geological Survey Professional Paper **774-C**.

Lockwood, J. P. and Lydon, P. A. (1975) *Geologic Map of the Mount Abbot Quadrangle, California*, 1:62 500. U.S. Geological Survey Map **GQ-1155**.

Martel, S. J., Pollard, D. D. and Segall, P. (1988) Development of simple strike-slip fault zones in granitic rock, Mount Abbot quadrangle, Sierra Nevada, California. *Bulletin of the Geological Society of America* **100**, 1451–1465.

Mitra, G. (1978) Ductile deformation zones and mylonites: The mechanical processes involved in the deformation of crystalline basement rocks. *American Journal of Science* **278**, 1057–1084.

Nicolas, A. and Poirier, J. P. (1976) *Crystalline Plasticity and Solid State Flow in Metamorphic Rocks*. John Wiley and Sons, New York.

Ohnaka, M. (1992) Earthquake source nucleation; a physical model for short-term precursors. *Tectonophysics* **211**, 149–178.

Passchier, C. W. (1982) Pseudotachylyte and the development of ultramylonite bands in the Saint-Barthelemy Massif, French Pyrenees. *Journal of Structural Geology* **4**, 69–79.

Passchier, C. W. (1986) Flow in natural shear zones—the consequences of spinning flow regimes. *Earth and Planetary Science Letters* **77**, 70–80.

Poirier, J. P. (1980) Shear localization and shear instability in materials in the ductile field. *Journal of Structural Geology* **2**, 135–142.

Prescott, W. H. and Nur, A. (1981) The accommodation of relative motion at depth on the San Andreas fault system in California. *Journal of Geophysical Research* **86**, 999–1004.

Prescott, W. H., Savage, J. C. and Kinoshita, W. T. (1979) Strain accumulation rates in the western United States between 1970 and 1978. *Journal of Geophysical Research* **84**, 5423–5435.

Ramsay, J. G. (1980) Shear zone geometry: a review. *Journal of Structural Geology* **2**, 83–99.

Ramsay, J. G. and Graham, R. H. (1970) Strain variations in shear belts. *Canadian Journal of Earth Sciences* **7**, 786–813.

Rudnicki, J. W. and Rice, J. R. (1975) Conditions for the localization of deformation in pressure-sensitive dilatant materials. *Journal of the Mechanics and Physics of Solids* **23**, 371–394.

Savage, J. C. and Burford, R. O. (1973) Geodetic determination of relative plate motion in central California. *Journal of Geophysical Research* **78**, 832–845.

Schmid, S. M. (1975) The Glarus overthrust: Field evidence and mechanical model. *Eclogae Geologicae Helvetiae* **68**, 257–291.

Scholz, C. H. (1988) The brittle–plastic transition and the depth of seismic faulting. *Geologische Rundschau* **77**, 319–328.

Segall, P., McKee, E. H., Martel, S. J. and Turrin, B. D. (1990) Late Cretaceous age of fractures in the Sierra Nevada batholith, California. *Geology* **18**, 1248–1251.

Segall, P. and Pollard, D. D. (1983) Nucleation and growth of strike-slip faults in granite. *Journal of Geophysical Research* **88**, 555–568.

Segall, P. and Simpson, C. (1986) Nucleation of ductile shear zones on dilatant fractures. *Geology* **14**, 56–59.

Sibson, R. H. (1977) Fault rocks and fault mechanisms. *Journal of the Geological Society of London* **33**, 191–213.

Sibson, R. H. (1980) Transient discontinuities in ductile shear zones. *Journal of Structural Geology* **2**, 165–171.

Sibson, R. H. (1982) Fault zone models, heat flow, and the depth distribution of earthquakes in the continental crust of the United States. *Bulletin of the Seismological Society of America* **72**, 151–163.

Simpson, C. (1983a) Strain and shape fabric variations associated with ductile shear zones. *Journal of Structural Geology* **5**, 61–72.

Simpson, C. (1983b) Displacement and strain patterns from naturally occurring shear zone terminations. *Journal of Structural Geology* **5**, 497–506.

Simpson, C. (1985) Deformation of granitic rocks across the brittle–ductile transition. *Journal of Structural Geology* **7**, 503–511.

Steiger, R. H. and Jäger, E. (1977) Subcommission on geochronology: Convention on the use of decay constants in geo- and cosmochronology. *Earth and Planetary Science Letters* **36**, 359–362.

Stern, T. W., Bateman, P. C., Morgan, B. A., Newall, M. F. and Peck, D. L. (1981) Isotopic U–Pb ages of zircon from the granitoids of the central Sierra Nevada, California. *U.S. Geological Survey Professional Paper* **1185**, 17.

Thatcher, W. (1975a) Strain accumulation and release mechanism of the 1906 San Francisco earthquake. *Journal of Geophysical Research* **80**, 4862–4872.

Thatcher, W. (1975b) Strain accumulation on the northern San Andreas fault zone since 1906. *Journal of Geophysical Research* **80**, 4873–4880.

Tse, S. T. and Rice, J. R. (1986) Crustal earthquake instability in relation to the depth variation of frictional slip properties. *Journal of Geophysical Research* **91**, 9452–9472.

Tullis, J. (1990) Experimental studies of deformation mechanisms and microstructure in quartzo-feldspathic rocks. In *Deformation Processes in Minerals, Ceramics and Rocks*, eds D. J. Barber and P. G. Meredith, pp. 190–227. Unwin Hyman, London.

Tullis, J., Dell'Angelo, L. and Yund, R. A. (1990) Ductile shear zones from brittle precursors in feldspathic rocks: The role of dynamic recrystallization. *American Geophysical Union, Geophysical Monograph* **56**, 67–81.

White, S. H., Burrows, S. E., Carreras, J., Shaw, N. D. and Humphreys, F. J. (1980) On mylonites in ductile shear zones. *Journal of Structural Geology* **2**, 175–187.

Wojtal, S. and Mitra, G. (1986) Strain hardening and strain softening in fault zones from foreland thrusts. *Bulletin of the Geological Society of America* **97**, 674–687.

Zoback, M. D., Prescott, W. H. and Krueger, S. W. (1985) Evidence for lower crustal ductile strain localization in southern New York. *Nature* **317**, 705–707.